

2

# NAVAL POSTGRADUATE SCHOOL Monterey, California

AD-A246 442



## THESIS



APPARATUS FOR MEASURING THE ABSORPTION  
OF SOUND BY NOISE IN ONE DIMENSION

by

Stephen J. Dorff

December, 1991

Co-Advisor  
Co-Advisor  
Co-Advisor

Bruce Denardo  
Andrés Larraza  
Anthony Atchley

Approved for public release; distribution is unlimited.

92 2 24 020

92-04596



Unclassified

SECURITY CLASSIFICATION OF THIS PAGE

REPORT DOCUMENTATION PAGE				Form Approved OMB No 0704 0188	
1a REPORT SECURITY CLASSIFICATION <b>Unclassified</b>			1b RESTRICTIVE MARKINGS		
2a SECURITY CLASSIFICATION AUTHORITY			3 DISTRIBUTION AVAILABILITY OF REPORT		
2b DECLASSIFICATION/DOWNGRADING SCHEDULE			Approved for public release; distribution is unlimited.		
4 PERFORMING ORGANIZATION REPORT NUMBER(S)			5 MONITORING ORGANIZATION REPORT NUMBER(S)		
6a NAME OF PERFORMING ORGANIZATION <b>Naval Postgraduate School</b>		6b OFFICE SYMBOL (If applicable) <b>33</b>	7a NAME OF MONITORING ORGANIZATION <b>Naval Postgraduate School</b>		
6c ADDRESS (City, State, and ZIP Code) <b>Monterey, CA 93943-5000</b>			7b ADDRESS (City, State, and ZIP Code) <b>Monterey, CA 93943-5000</b>		
8a NAME OF FUNDING SPONSORING ORGANIZATION		8b OFFICE SYMBOL (If applicable)	9 PROCUREMENT INSTRUMENT IDENTIFICATION NUMBER		
8c ADDRESS (City, State, and ZIP Code)			10a SOURCE OF FUNDING NUMBERS		10b WORK UNIT ACCESSION NO
			PROGRAM ELEMENT NO		PROJECT NO
			TASK NO		
11 TITLE (Include Security Classification) <b>APPARATUS FOR MEASURING THE ABSORPTION OF SOUND BY NOISE IN ONE DIMENSION</b>					
12 PERSONAL AUTHOR(S) <b>Stephen J. Dorff</b>					
13a TYPE OF REPORT <b>Master's Thesis</b>		13b TIME COVERED FROM _____ TO _____		14 DATE OF REPORT (Year, Month, Day) <b>December 1991</b>	
15 PAGE COUNT <b>40</b>					
16 SUPPLEMENTARY NOTES <b>The views expressed in this thesis are those of the author and do not reflect the official policy or position of the Department of Defence or the U.S. Government.</b>					
17 COSATI CODES			18 SUBJECT TERMS (Continue on reverse if necessary and identify by block number)		
FIELD	GROUP	SUB GROUP			
			<b>Nonlinear Acoustics, Finite Amplitude Propagation</b>		
19 ABSTRACT (Continue on reverse if necessary and identify by block number)					
<p>A travelling wave tube for the study of high intensity acoustics has been constructed. The tube has inner diameter two inches and length 70 feet, and consists of seven 10 foot long sections smoothly joined by collars and flanges. Attached to one end is a housing that contains two JBL horn drivers connected to the tube by a "Y" adapter. An anechoic end termination spans the length of the last section. The termination is made of steel wool of tapered density distribution. Pulse reflection measurements yielded an absorption of 40 dB or greater for frequencies of 500 Hz and higher. Reflected signals of the junctions were typically 40 dB down. Linear attenuation measurements indicated no appreciable acoustic losses at the junctions. Sum, difference and second harmonic generation measurements revealed that interactions were occurring in the medium of interest (air) and were not the result of the drivers or intermodulations of the two drivers. The performance under these preliminary tests indicates that the apparatus is suitable for nonlinear acoustics investigations.</p>					
20 DISTRIBUTION AVAILABILITY OF ABSTRACT			21 ABSTRACT SECURITY CLASSIFICATION		
<input type="checkbox"/> UNCLASSIFIED/UNLIMITED <input type="checkbox"/> SAME AS RPT <input type="checkbox"/> DTIC USERS			<b>Unclassified</b>		
22 NAME OF RESPONSIBLE INDIVIDUAL <b>B. Demardo</b>			23 TELEPHONE (Include Area Code) <b>(408)646-3485</b>		24 OFFICE SYMBOL <b>Ph-De</b>

Approved for public release; distribution is unlimited.

Apparatus for Measuring the Absorption of Sound  
by Noise in One Dimension

by

Stephen J. Dorff  
Lieutenant, United States Navy  
B.S., University of Cincinnati, 1983

Submitted in partial fulfillment  
of the requirements for the degree of

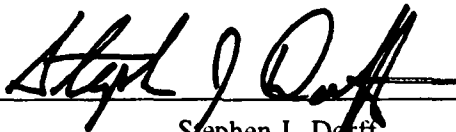
MASTER OF SCIENCE IN ENGINEERING ACOUSTICS

from the

NAVAL POSTGRADUATE SCHOOL

December 1991

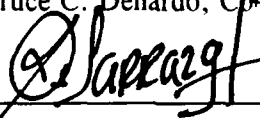
Author:

  
Stephen J. Dorff

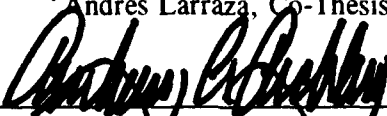
Approved by:



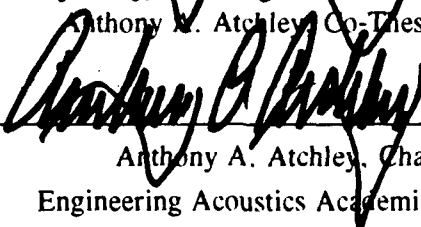
Bruce C. Denardo, Co-Thesis Advisor



Andrés Larraza, Co-Thesis Advisor



Anthony A. Atchley, Co-Thesis Advisor



Anthony A. Atchley, Chairman  
Engineering Acoustics Academic Committee

## ABSTRACT

A travelling wave tube for the study of high intensity acoustics has been constructed. The tube has inner diameter two inches and length 70 feet, and consists of seven 10 foot long sections smoothly joined by collars and flanges. Attached to one end is a housing that contains two JBL horn drivers connected to the tube by a "Y" adapter. An anechoic end termination spans the length of the last section. The termination is made of steel wool of tapered density distribution. Pulse reflection measurements yielded an absorption of 40 dB or greater for frequencies of 500 Hz and higher. Reflected signals of the junctions were typically 40 dB down. Linear attenuation measurements indicated no appreciable acoustic losses at the junctions. Sum, difference and second harmonic generation measurements revealed that interactions were occurring in the medium of interest (air) and were not the result of the drivers or intermodulations of the two drivers. The performance under these preliminary tests indicates that the apparatus is suitable for nonlinear acoustics investigations.



iii

<b>Accession For</b>	
NTIS GRA&I	<input checked="" type="checkbox"/>
DTIC TAB	<input type="checkbox"/>
Unannounced	<input type="checkbox"/>
Justification	
By	
Distribution/	
Availability Codes	
Dist	and/or Special
A-1	

## TABLE OF CONTENTS

I.	INTRODUCTION . . . . .	1
II.	THEORY . . . . .	3
	A. MODEL EQUATION OF MOTION . . . . .	3
	B. PERTURBATION APPROACH . . . . .	4
	C. GENERATION OF SUM AND DIFFERENCE PROCESS . . . . .	7
III.	APPARATUS . . . . .	13
	A. DRIVER SELECTION . . . . .	13
	B. TUBE DESIGN AND CONSTRUCTION . . . . .	15
	C. ABSORBER DESIGN AND PERFORMANCE . . . . .	22
	D. MICROPHONE PORTS . . . . .	25
	E. EXPERIMENTAL TESTS . . . . .	27
IV.	SUMMARY AND CONCLUSIONS . . . . .	32
	REFERENCES . . . . .	34
	INITIAL DISTRIBUTION LIST . . . . .	35

## I. INTRODUCTION

A small amplitude acoustic signal in the presence of large amplitude broad band noise attenuates due to nonlinear interaction with the entire band. If the noise is isotropic, the attenuation is exponential. This was predicted by Westervelt 1976 and later observed in sound in water (Stanton and Beyer, 1978). If the interaction is restricted to be in one dimension, the attenuation has been predicted to be no longer exponential (Rudenko and Chirkin, 1975). This remarkable behavior and the required degree of anisotropy of the noise for the behavior to persist have not been investigated by previous researchers. Moreover, the physical implications of this result have not been explored.

The non-exponential nature of the attenuation reveals a breaking of translational invariance of the underlying system, establishes the existence of nonlocal fluctuating forces, disallows an associated H-theorem for the system of interacting waves, and is indicative of a far off equilibrium behavior. The transition to an exponential behavior as a function of anisotropy of the noise is of interest because it is unclear how such transition should occur, or whether in some sense, it can be characterized as a phase transition.

The purpose of this thesis is to describe the design, construction, and preliminary tests of a high intensity travelling acoustic wave tube. The apparatus will be used to

experimentally investigate the attenuation of a weak acoustic signal in the presence of high intensity broad band acoustic noise in one dimension.

The organization of this thesis is as follows. Chapter II presents a perturbative approach to the derivation of the attenuation of an impressed wave in a background of noise in one dimension. Concerns about the intermodulation of the two drives demanded the experimental investigation of sum, difference, and harmonic frequency generation. The last section of Chapter II presents the theory for these processes so that a comparison of the data can be established. Chapter III details the design, construction, and preliminary testing of the apparatus. Chapter IV is a summary of the results and conclusions.

## II. THEORY

### A. MODEL EQUATION OF MOTION

The basic nonlinear interaction for acoustic waves is a three wave resonance, so that waves with frequencies  $\omega_1$  and  $\omega_2$  scatter to produce waves with frequencies  $\omega_3 = \omega_1 \pm \omega_2$ . Furthermore, because these waves are dispersionless the interactions can only be collinear.

For random waves in two and three dimensions energy in the noise components redistributes irreversibly by collinear resonant interaction. Randomization in angle is brought about by slower collision processes whereby redistribution occurs by a local transfer between adjacent rays (Newell and Aucoin, 1971). Thus, a closed system of interacting random waves can after a time determined by nonlinearities, reach thermodynamic equilibrium and small fluctuations about steady states relax exponentially.

The approach to equilibrium for waves in one dimension remains an open question. Analogous to the two and three dimensional case (Cabot, 1983), we can investigate some of the features of the problem by considering the basic interaction of an acoustic signal and a background of noise.

Because the basic nonlinear interaction is three wave resonance of collinear waves, we can without loss of generality consider a model equation for unidirectional

propagation of the disturbance  $\rho$  about its equilibrium value  $\rho_0$  with quadratic nonlinearities

$$(\partial_t + c \partial_x) \rho = -\frac{Gc}{2\rho_0} \partial_x \rho^2, \quad II.A.1$$

where  $c$  is the equilibrium value for the speed of sound and

$$G = 1 + \frac{\rho}{c} \frac{dc}{d\rho} \quad II.A.2$$

is the Gruneissen coefficient which results from considerations of Galilean covariance (the first term) and the leading nonlinear term in the equation of state (the second term).

Normalizing such that  $x \Rightarrow x/c$  and  $\rho \Rightarrow (G/\rho_0)^{1/2} \rho$  we get

$$(\partial_t + \partial_x) \rho = -\rho \partial_x \rho. \quad II.A.3$$

Equation II.A.3 constitutes the lowest order nonlinear model equation for unidirectional propagation. It will be the basis for our investigations of nonlinear interaction of sound by noise.

## B. PERTURBATION APPROACH

Here we analyze the evolution of an infinitesimal continuous wave in a background of noise. We will not consider self interaction effects nor redistribution of energy among noise components.

Let us now begin a straightforward perturbation expansion for the solution of equation II.A.3

$$\rho = \epsilon \rho_1 + \epsilon^2 \rho_2 + \epsilon^3 \rho_3 + \dots \quad II.B.1$$

Thus the different orders obey the equations

$$O(\epsilon) : \quad (\partial_t + c \partial_x) \rho_1 = 0 \quad , \quad II.B.2a$$

$$O(\epsilon^2) : \quad (\partial_t + c \partial_x) \rho_2 = -\frac{1}{2} \partial_x \rho_1^2 \quad , \quad II.B.2b$$

$$O(\epsilon^3) : \quad (\partial_t + c \partial_x) \rho_3 = -\partial_x \rho_1 \rho_2 \quad . \quad II.B.2c$$

An impressed wave and a background of noise satisfy equation II.B.2a, that is

$$\rho_1 = a e^{ikx - i\omega t} + \sum_q \rho_q e^{iqx - i\Omega t} + c.c. \quad , \quad II.B.3$$

provided

$$\omega = k \quad , \quad \Omega(q) = q \quad . \quad II.B.4$$

Because we are not considering redistribution of energy among noise components, the  $\rho_q$  is undepleted and no energy flows back and forth between noise and impressed wave.

This means that the relevant terms for  $\rho_1^2$  in equation II.B.2b are (sum over  $q$  can be omitted)

$$\rho_1^2 = 2a\rho_q e^{i(k+q)x - i(\omega+\Omega)t} + 2a\rho_{-q} e^{i(k-q)x - i(\omega-\Omega)t} + c.c. \quad . \quad II.B.5$$

Thus

$$-\partial_x \rho_1^2 = -2ia[(k+q)\rho_q e^+ + (k-q)\rho_{-q} e^-] + c.c. \quad II.B.6$$

where  $e^\pm = e^{i(k\pm q)x - i(\omega\pm\Omega)t}$ . A particular solution is the secular expression

$$\rho_2 = a(\alpha x e^+ + \beta x e^-) + c.c. \quad II.B.7$$

Applying this solution to equation II.B.2b we find the values

$$\alpha = -i(k+q)\rho_q \quad ; \quad \beta = -i(k-q)\rho_{-q} \quad II.B.8$$

We now consider the third order terms, and include only those terms that resonantly drive the contribution of the third order density to the impressed wave, that is, the term

$$-\partial_x \rho_1 \rho_2 = -2ak^2 |\rho_q|^2 x e^{i(kx-i\omega t)} - 2iak |\rho_q|^2 e^{ikx-i\omega t} \quad II.B.9$$

resonantly drives the left hand side of equation II.B.2c. Thus, the solution

$$\rho_3 = -(ak^2 |\rho_q|^2 x^2 + 2iak |\rho_q|^2 x) e^{ikx-i\omega t} \quad II.B.10$$

satisfies the third order equation. Incorporating the contribution from all the noise components, the impressed wave evolves according to

$$\rho = a(1 - 2ikx \sum_q |\rho_q|^2 - k^2 x^2 \sum_q |\rho_q|^2) e^{ikx-i\omega t} \quad II.B.11$$

This solution can be interpreted as the first order Taylor expansion of

$$\rho = a e^{-k^2 x^2 \sum_q |\rho_q|^2} e^{ikx(1 - 2 \sum_q |\rho_q|^2 x) - i\omega t}, \quad II.B.12$$

corresponding to attenuation due to the integrated noise energy as well as a frequency shift.

Unlike the two and three dimensional problems for which the attenuation of an impressed wave is exponential, the one dimensional case yields a gaussian attenuation in

agreement with Rudenko and Chirkin (1975). This fundamentally different result might contain the clue to the understanding of whether a one dimensional system can approach equilibrium. In addition, the result has not been tested experimentally.

### C. GENERATION OF SUM AND DIFFERENCE PROCESS

Because the attenuation of a wave due to a background of noise depends on nonlinear interactions, a fundamental test is to determine that these interactions happen in the medium and not in the transducers. In this section we consider the theory of generation of sum and difference frequencies due to monochromatic sources. Rather than using the model equation II.A.1, we shall use the actual equations of motion. This stems from the fact that the nature of the source and the detector are important, (see II.C.11), because the relation between dynamical variables (pressure, velocity) is nonlinear.

The speed of propagation of a unidirectional disturbance in a gas medium is (Riemann, 1858)

$$u = c_0 + \frac{\gamma+1}{2} v \quad , \quad II.C.1$$

where  $v$  is the particle velocity and  $c_0$  is the equilibrium value of the speed of sound.

Thus the exact equation of motion for unidirectional propagation is

$$\frac{\partial v}{\partial t} + (c_0 + \frac{\epsilon}{2} v) \frac{\partial v}{\partial x} = 0 \quad , \quad II.C.2$$

where  $\epsilon = (\gamma+1)/2$ . Note the similarity of equation II.C.2 to our model equation

II.A.3. Consider a two-frequency disturbance at  $x = 0$

$$v = v_{01} \cos \omega_1 t + v_{02} \cos \omega_2 t \quad , \quad II.C.3$$

where the amplitudes  $v_{01}$  and  $v_{02}$  are small. We can employ a perturbation approach for the velocity field in the form

$$v = v^{(1)} + v^{(2)} + \dots \quad , \quad II.C.4$$

where  $v^{(i)}/v^{(i-1)} = O(\mu)$  and  $\mu$  is a small parameter.

We also transform to a coordinate system moving with the wave. Distortions of the profile of the wave are small over distances of the order of a wavelength. Thus  $v$  should be written as a function of the form

$$v = v\left(t - \frac{x}{c_0}, \mu x\right) \quad . \quad II.C.5$$

Equation II.C.3 then becomes

$$\frac{\partial v}{\partial x} = \frac{\epsilon}{c_0^2} v \frac{\partial v}{\partial \tau} \quad II.C.6$$

where  $\tau = t - x/c_0$ .

The solution to II.C.6 that describes the propagation of a first order velocity field radiated by a surface that is oscillating according to II.C.4 can be written in the form

$$v^{(1)} = v_{01} \cos \omega_1 \tau + v_{02} \cos \omega_2 \tau \quad . \quad II.C.7$$

Substituting II.C.7 in the right side of II.C.6, we get

$$\frac{\partial v^{(2)}}{\partial x} = - \frac{\epsilon v_{01} v_{02} \omega_1}{2 c_0^2} \sin \omega_1 \tau \quad , \quad II.C.8a$$

$$\frac{\partial v_-^{(2)}}{\partial x} = -\frac{\epsilon v_{01} v_{02} \omega_-}{2c_o} \sin \omega_- \tau, \quad II.C.8b$$

for the sum and difference processes respectively, with  $\omega_{\pm} = \omega_1 \pm \omega_2$ . Equations II.C.8 have solutions of the form

$$v_+^{(2)} = -\frac{\epsilon \omega_+ v_{01} v_{02}}{2c_o^2} x \sin \omega_+ \tau, \quad II.C.9a$$

$$v_-^{(2)} = -\frac{\epsilon \omega_- v_{01} v_{02}}{2c_o^2} x \sin \omega_- \tau. \quad II.C.9b$$

Up to quadratic terms the acoustic pressure is

$$\frac{p}{p_o} = 1 + \gamma \frac{v}{c_o} + \gamma \frac{\gamma+1}{4} \frac{v^2}{c_o^2}. \quad II.C.10$$

So we see that pressure measurements will detect sum and difference processes at the velocity source. One should then have knowledge of the nature of the source for this will affect calibration sensitivity.

The pressure equation, valid up to second order, is

$$\frac{\partial p}{\partial x} = \frac{\epsilon}{c_o \gamma} \frac{p}{p_o} \frac{\partial p}{\partial \tau}. \quad II.C.11$$

The replacement  $\epsilon/c_o^2 \rightarrow \epsilon/(c_o \gamma p_o)$  yields, for a pressure drive the expressions

$$p_{\pm}^{(2)} = -\frac{\epsilon \omega_{\pm} p_{01} p_{02}}{2c_o \gamma p_o} x \sin \omega_{\pm} \tau, \quad II.C.12$$

where  $p_o$  is the atmospheric pressure. Next, we include a phenomenological dissipative term representing losses at the wall

$$\frac{\partial p}{\partial x} + \alpha p = \frac{\epsilon p}{c_o \gamma p_o} \frac{\partial p}{\partial \tau} \quad , \quad II.C.13$$

where

$$\alpha = \beta \omega^{1/2} \quad , \quad II.C.14$$

Note the nonanalytic frequency dependence of the attenuation coefficient  $\alpha$ .

The first order solution to II.C.13 that describes the propagation of a pressure wave radiated by a surface that is oscillating according to

$$p^{(1)} = p_{01} \cos \omega_1 \tau + p_{02} \cos \omega_2 t \quad II.C.15$$

is given by

$$p^{(1)} = p_{01} e^{-\alpha_1 x} \cos \omega_1 \tau + p_{02} e^{-\alpha_2 x} \cos \omega_1 \tau \quad . \quad II.C.16$$

Substituting II.C.16 into the right hand side of II.C.13 we get

$$\frac{\partial p^{(2)}}{\partial x} + \alpha_+ p^{(2)} = - \frac{\epsilon p_{01} p_{02} \omega_+}{2 c_o \gamma p_o} e^{-(\alpha_1 + \alpha_2) x} \sin \omega_+ \tau \quad . \quad II.C.17$$

The solution to II.C.17 consists of the sum of the particular solution and the general solution of the homogenous equation with boundary condition  $p^{(2)}=0$  at  $x=0$ . One gets

$$p^{(2)} = [e^{-(\alpha_1 + \alpha_2) x} - e^{-\alpha_+ x}] \frac{\epsilon p_{01} p_{02} \omega_+}{2 (\alpha_1 + \alpha_2 - \alpha_+) c_o \gamma p_o} \sin \omega_+ \tau \quad . \quad II.C.18$$

The maximum pressure is at

$$x_{\max}^{(\pm)} = \ln\left(\frac{\alpha_1 + \alpha_2}{\alpha_{\pm}}\right) \frac{1}{\alpha_1 + \alpha_2 - \alpha_{\pm}} \quad . \quad II.C.19$$

For a trial run with  $f_1 = 750$  Hz,  $f_2 = 2000$  Hz, we get the theoretical values  $x_{\max}^+ = 14.26$  meters,  $x_{\max}^- = 17.33$  meters.

If we have a velocity drive, the second order pressure is given by

$$\frac{p^{(2)}}{p_o} = \gamma \frac{v^{(2)}}{c_o} + \gamma \frac{\gamma+1}{4} \left( \frac{v^{(1)}}{c_o} \right)^2 \quad . \quad II.C.20$$

The velocity of the sum and difference due to a velocity drive is

$$v_{\pm}^{(2)} = \{e^{-(\alpha_1 + \alpha_2)x} - e^{-\alpha_{\pm}x}\} \frac{\epsilon V_{01} V_{02} \omega_{\pm}}{2(\alpha_1 + \alpha_2 - \alpha_{\pm}) c_o^2} \sin \omega_{\pm} \tau \quad . \quad II.C.21$$

Thus the pressure for the sum and difference due to a velocity drive is given, according to II.C.20

$$\begin{aligned} \left( \frac{p^{(2)}}{p_o} \right)_{\pm} &= \gamma \{e^{-(\alpha_1 + \alpha_2)x} - e^{-\alpha_{\pm}x}\} \frac{\epsilon V_{01} V_{02} \omega_{\pm}}{2(\alpha_1 + \alpha_2 - \alpha_{\pm}) c_o^3} \sin \omega_{\pm} \tau \\ &+ \gamma e^{-(\alpha_1 + \alpha_2)x} \frac{\epsilon V_{01} V_{02}}{2 c_o^2} \cos \omega_{\pm} \tau \quad . \quad II.C.22 \end{aligned}$$

In terms of pressure amplitudes II.C.23 becomes

$$\begin{aligned}
P_{\pm}^{(2)} = & \left\{ e^{-(\alpha_1 + \alpha_2)x} - e^{-\alpha_{\pm}x} \right\} \frac{\epsilon P_{01} P_{02} \omega_{\pm}}{2(\alpha_1 + \alpha_2 - \alpha_{\pm}) \gamma P_0 c_0} \sin \omega_{\pm} \tau \\
& + e^{-(\alpha_1 + \alpha_2)x} \frac{\epsilon P_{01} P_{02}}{2 P_0 \gamma} \cos \omega_{\pm} \tau, \quad II.C.23
\end{aligned}$$

which is a valid expression up to  $O(\mu^2)$ , with  $\alpha_i = O(\mu)$  quantities. For small distances, or equivalently for no dissipation,

$$P_{\pm}^{(2)} = - \frac{\epsilon P_{01} P_{02}}{2 P_0 \gamma} \left\{ \frac{\omega_{\pm} x}{c_0} \sin \omega_{\pm} \tau - \cos \omega_{\pm} \tau \right\}, \quad II.C.24$$

which has the same growth rate as the pressure (II.C.12) for a pressure drive.

### III. APPARATUS

This chapter discusses the design and construction of the experimental apparatus and test results. The apparatus must produce and convey finite amplitude one dimensional propagation of sound in air. High intensity travelling waves can give rise to vortex production at nonuniformities and uneven surfaces. To prevent this, a propagation tube for nonlinear waves must be made with a higher degree of smoothness than is the usual case with linear waveguides. Round aluminum pipe is used since a circular cross section provides no corners that might needlessly complicate or distort the sound field. All junctions, microphone ports and adaptor seals must be sufficiently tight to ensure little leakage of sound intensity out of the tube. High output compression drivers are needed to produce a finite amplitude noise source. Finally, a high performance absorbing termination is required because we desire unidirectional travelling waves.

#### A. DRIVER SELECTION

We selected JBL models 2445H/J compression drivers as the primary sources. A JBL 2485J was purchased in the event more power was needed at lower frequency. Models 2445H/J are titanium diaphragm drivers rated at 100 watts from 500 to 1000Hz and 150 watts above 1000Hz. Model 2485J is a phenolic diaphragmed driver rated at 120 watts from 300 to 1000Hz and 150 watts above a kilohertz. Given these

performance criteria and our high power requirement, it is evident that operation must be at frequencies greater than roughly 500 Hz.

The drivers were mounted to a 2-to-1 driver horn throat adapter (JBL #2329) which was mounted to a 1-to-1 throat adapter (JBL #2328). These two connected adapters converted the assembly to a standard JBL two inch inner diameter flanged junctions at both the input and output ends so that drivers and the tube could be connected.

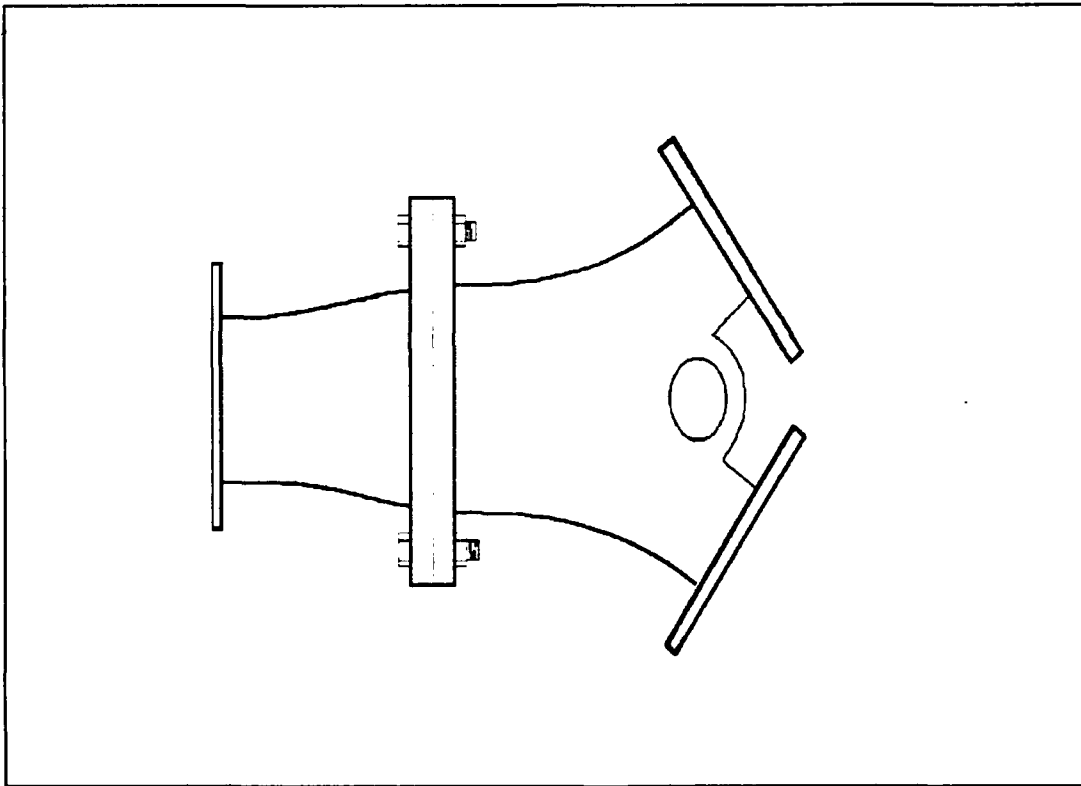


**Figure 1:** Twin driver coupling to propagation tube using two JBL horn throat adapters.

Beyond this "Y" assembly, the only nonuniformities seen by the wave train will be those within the pipe. The driver assembly was mounted in a sturdy box for protection from accidental bumps, to provide physical support, to facilitate the mounting of fuses and power junctions, and to reduce the possibility of theft. The box has no intended or observed acoustic effect and does not constitute a driver baffle.

## **B. TUBE DESIGN AND CONSTRUCTION**

Factors influencing the choice of tube material and dimensions were: (a) A sufficiently high cutoff frequency so that only plane waves will exist for the experimental frequency region. (b) Easy machining and absorber installation. (c) Availability; we wanted to select off-the-shelf pipe from a local supplier. (d) Weight; the entire apparatus is designed for mounting on a corridor wall and must not be so heavy as to make handling and mounting difficult. (e) Wall thickness should be sufficiently large to reduce radiation and allow threaded microphone ports.

The best solution to all of these criteria was determined to be extruded aluminum pipe of about 2 inches inner diameter and 2 3/8 inches outer diameter. The actual average inner diameter of the pipes received was  $1.957 \pm 0.004$  inches. The average outer diameter was  $2.377 \pm 0.005$  inches. The frequency of the first transverse mode in air at 20° C is approximately (Kinsler et al, 1982)

$$f_{1,1} \approx \frac{101}{r} \quad . \quad III.B.1$$

where  $f_{1,1}$  is in Hz and the radius  $r$  is in meters. This gives a cut-off frequency of 4064 Hz. Only plane waves can propagate below this frequency. From this and the characteristics of the compression drivers discussed in section III.B, it is clear that the frequency region accessible for plane wave experimentation is about 500 to 4,000 Hz.

The length of the tube is determined by the distance required to observe the sound on sound absorption and the length needed for an efficient absorber. Although the sound on sound absorption effect is expected to be observable within the first twenty feet of propagation, we decided to provide sixty feet of usable tube before the absorber section. This provides ample length in the event our estimates prove optimistic and also places the absorber several meters away from where we intend to make most of our observations. Here an effort was made to construct the tube so that follow-on experiments are possible without major modification. Maintaining a smooth and even surface down the interior of the tube required junction couplings that would reliably align, join, and seal the machined ends of the pipe sections. The pipe was purchased in 20 foot lengths but for ease of handling these were cut in half. Maximum inner diameters and minimum outer diameters determined from the lot were 1.963 inches and 2.370 inches, respectively. Using these values we decided to machine the inner and outer end surfaces to 1.975 and 2.340 inches to ensure that metal would be removed in the machining process and thus provide a machined fit. The ends of the pipe sections were faced flat and the outer cylindrical surface turned down to uniform 2.340 inches

diameter extending 3.25 inches from the ends. The inside of the pipe begins with a 1.975 initial diameter (at the very edge of the pipe section) and decreases on a one degree taper into the pipe section interior.

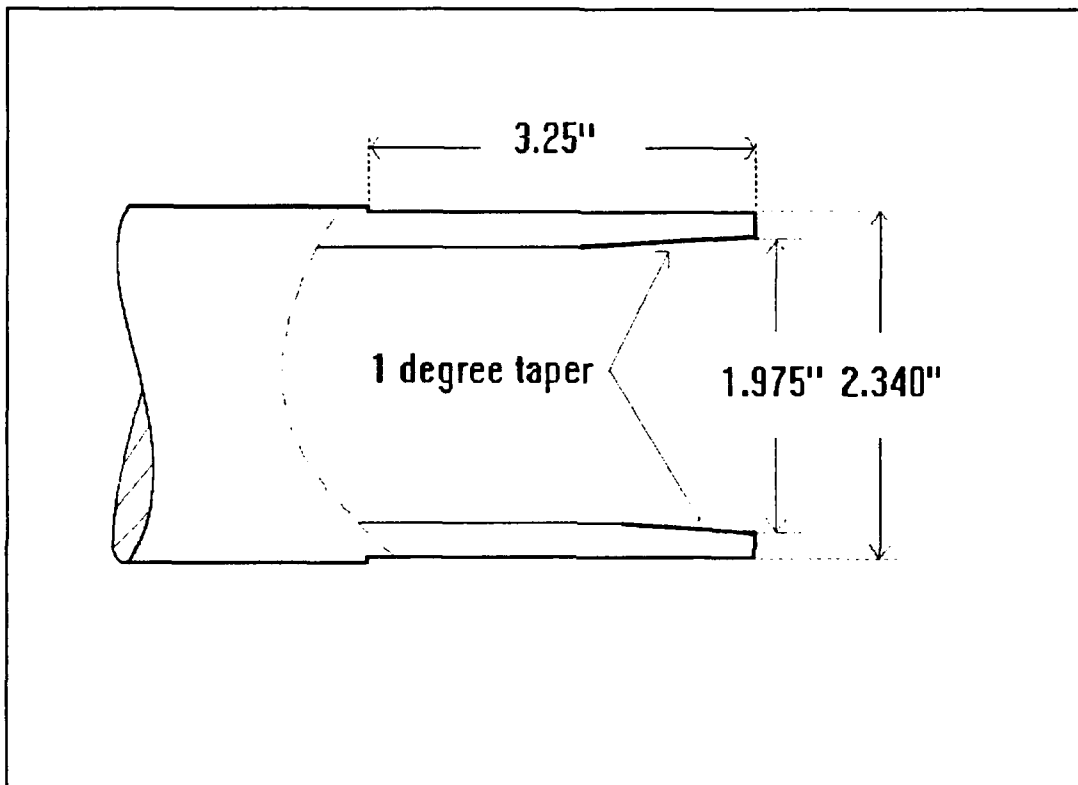


**Figure 2:** Pipe end machining details.

Each pipe end now has an equal inner diameter centered on the machined 2.340 inch outer diameter so that when butted together there is no appreciable step or uneven edge across the junction. The slightly tapered inner surface provides a smooth transition across the junction with only a 2% average change in cross sectional area.

Brass sleeves 3 inches long, 2.341 inches inner diameter, and about 3.5 inches outer diameter were employed to couple and maintain alignment of the sections.

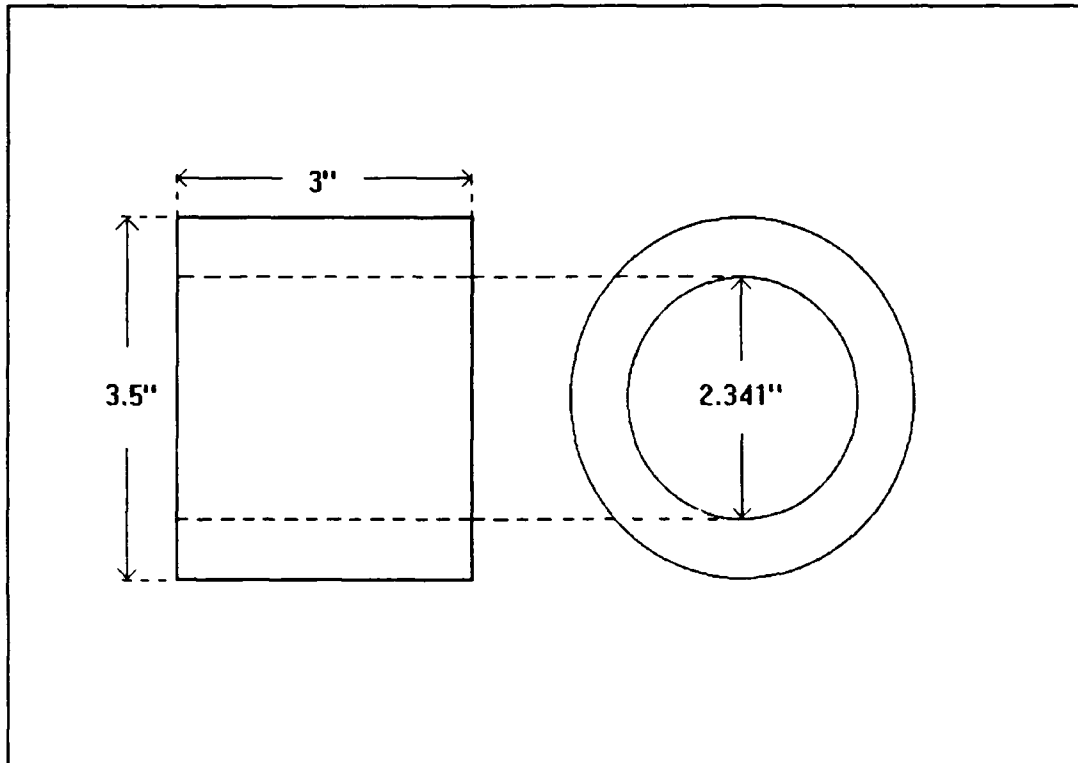


**Figure 3:** Sliding sleeve design used to maintain alignment of pipe ends.

Brass was used to prevent galling between the pipe sections and sleeve. A clearance of 0.001 inch was chosen so the sleeve could be slid by hand on the pipe ends while retaining a snug fit. Since the machined outer surfaces of the pipe sections were 3.25 inches long, a total of 6.5 inches of uniform machined outer surface was available at each junction. With this machined length, the brass sleeve could be pushed completely

onto the end of one section, fully exposing the gap between the pipes. This was a convenient way to check the alignment of the tube when mounted. With the sleeve all the way to one side, one could observe the gap between the end faces of the pipe sections and see the slight differences in this gap width over different sides of the tube. The sections could then be carefully moved to provide a flush fit and the sleeve was then slid back into place. A very fine feeler gauge could be used, but practice showed that the unassisted eye worked well and obviated the use of invasive instruments that might scratch machined surfaces. Split flanges were used to keep the pipe ends butted tightly together. With the sleeve positioned over the middle of the junction there remains 1.75 inches of outer machined surface exterior to the sleeve on which to place the split flanges. We constructed these flanges from 1.0 inch thick aluminum plate with a center bore that was the same (2.340 inches) as the pipe section's outer machined surfaces. When cut in half (see Figure 4) the flange fits the surface precisely as both have the same radius of curvature. The flange is then tightened with two 4.5 inch long  $\frac{3}{8}$  inch bolts. Six  $\frac{3}{8}$  inch bolts of 6 inches length span across the sleeve to another flange to provide the force necessary to keep the pipe sections butted together inside the sleeve.

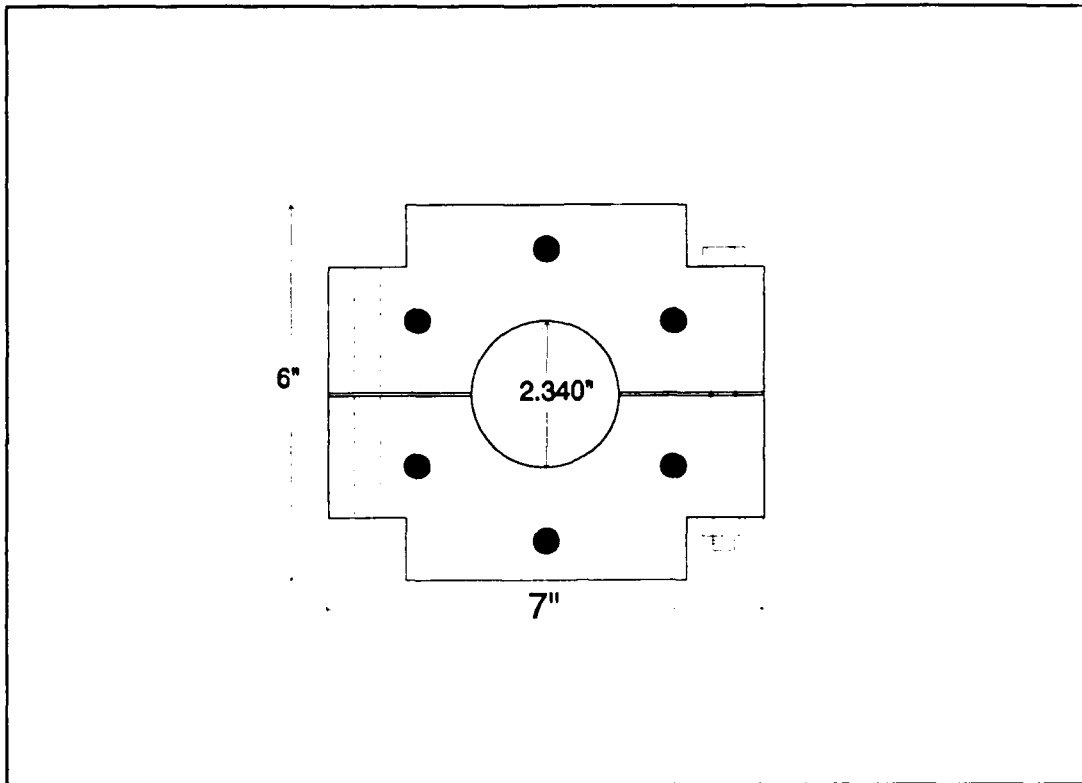


**Figure 4:** Split flange design.

An adapter was constructed to convert the 2 inch flanged coupling of the JBL throat adapters to a junction of the same design used for the pipe sections. (See Figure 5). This adaptor was machined from 5 inch round aluminum stock and is 5 inches long. The outer surface of its output side is 2.340 inches in diameter and is joined to the rest of the tube in the same manner as the pipe sections using a brass sleeve and two split flanges.

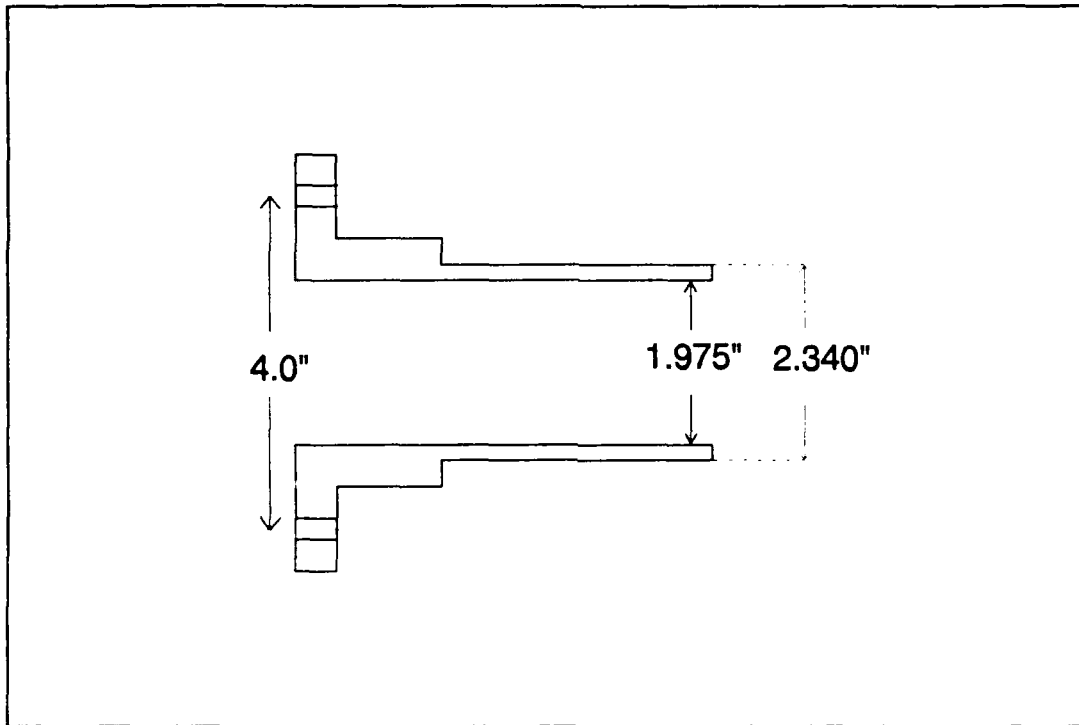


**Figure 5:** Adapter made to join "Y" assembly to propagation tube flanges.

The entire apparatus was mounted to a long corridor wall using Unistrut Corporation channel and brackets. The wall channel was 15 inches long and was held to the wallboard with three heavy toggle bolts. Two supports were used per pipe section. At the driver end, where the weight of the apparatus is greatest, two five foot lengths of channel were used to support the driver box. The length of the tube spanned a transition from a concrete to a wallboard wall. By choosing an appropriate wall position the long channel pieces supporting the drivers were mounted with three fasteners to the concrete wall so that greater strength was provided here. The brackets can be slid up and down on the wall channel and tightened in place providing vertical movement for alignment. These brackets are of the same channel material and pipe straps bolted onto them can be

loosened and slid horizontally. These two free directions allow proper tube alignment. A durable and dense foam rubber made by WALLIMCOA to thermally insulate pipes was used for vibration and acoustic isolation between the tube and the pipe straps.

### C. ABSORBER DESIGN AND PERFORMANCE

A high performance absorbing termination was needed to ensure that unidirectional propagating waves were dominant within the tube. Super fine steel wool (grade 0000) was used as the absorbing material. Absorber design was done following the work of Stephen Burns (1971) who modeled the absorptive process of fibrous material and conducted specific measurements for grade 0000 steel wool. By assuming that an ideal absorbing termination should present a small but constant change per length in acoustic impedance to minimize reflection, Burns showed that the ideal density distribution of wool with respect to distance down the pipe is

$$\rho(x) = [ (d\rho/dx)_{x=0} / k_a ]^{1/2} \tan [ (d\rho/dx)_{x=0} k_a ]^{1/2} x , \quad III.C.1$$

where  $x$  is the position along the pipe which begins at  $x = 0$ ,  $\rho$  is the density of steel wool in  $\text{grams/cm}^3$ , and  $k_a$  has units of  $(\text{Np/m})/(\text{gm/cm}^3)$  and is the absorption coefficient of the wool divided density ( $\alpha = k_a \rho(x)$ ). Burns demonstrated that a reflection amplitude of only -40 dB was possible for the tangent taper. This was the performance criteria chosen for our apparatus. After the final maximum density of wool is reached at distance  $x_n$ , the end of the taper, a uniform section of wool continues to the end of the tube. (See Figure 6).

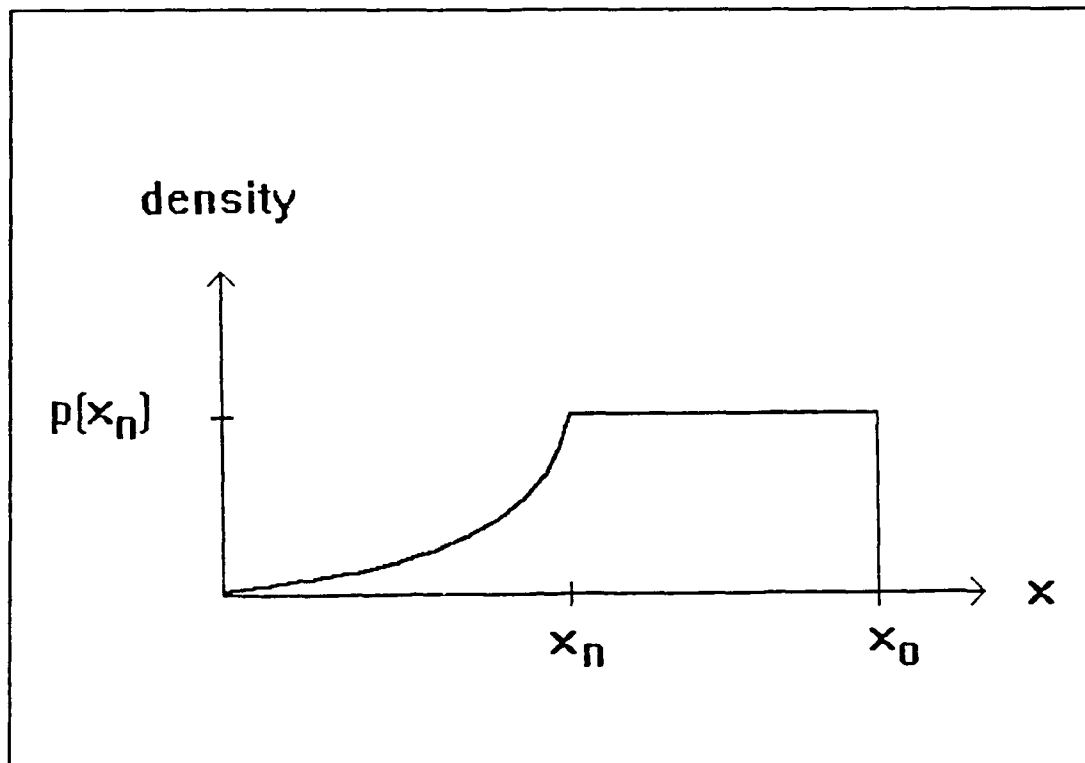


Figure 6: Tangent wedge absorber design.

The length of this uniform section depends upon the acceptable amount of reflection that can be tolerated from the open end. Following Burns' suggestion, reflections from the open end were desired to be only ten percent as large as those off the tangent taper and therefore negligible. This required the end reflections to be 0.1% the amplitude of the incident wave. Given test results from Burns' experiments, a full wavelength taper of one meter length ( $x_n = 1$ ) was used to provide efficient absorption above 343 Hz. The required length of the uniform density section is found by choosing  $TWT_{\text{uniform}}$  (the two

way transmission amplitude reduction) to be 0.001, setting  $x_n$  equal to 1, and solving for  $x_0$  in the following equation:

$$TWT_{uniform} = \exp(-2k_{\alpha} \rho(x_n) [x_0 - x_n]) \quad . \quad III.C.2$$

Burns determined  $k_{\alpha}$  to be 90 at 480 Hz with an approximate frequency dependence of  $f^{0.31}$ . By extrapolation 81 is obtained for 343 Hz. Using this value in the above equation gives  $x_0 = 1.74$  meters, or 0.74 meters of uniform density wool after the one meter taper. Performance tests using pulse bursts from 500 to 4,000 Hz showed that an excessive end reflection was still present and was possibly due to a slight bunching of the wool in the neighborhood of two string loops used to insert the wool into the tube. The uniform section was lengthened to 2.05 meters ( $x_0 = 3.05$  meters or about 10 feet) and no reflection from the open end was detectable. The total absorber length of ten feet fully occupies the last pipe section. This is a convenient configuration because the absorber can be easily removed from the tube assembly. The performance of the absorber was very good and is shown versus frequency in Figure 7. The reflection amplitude is less than 1% of the incident amplitude for frequencies from 600 to 4,000 Hz, and less than 2% of the incident amplitude for frequencies between 400 and 600 Hz. The reflections from the junctions were -44 dB or lower for the entire range of frequencies and exceeded absorber reflection from 2300 to 3900 Hz.

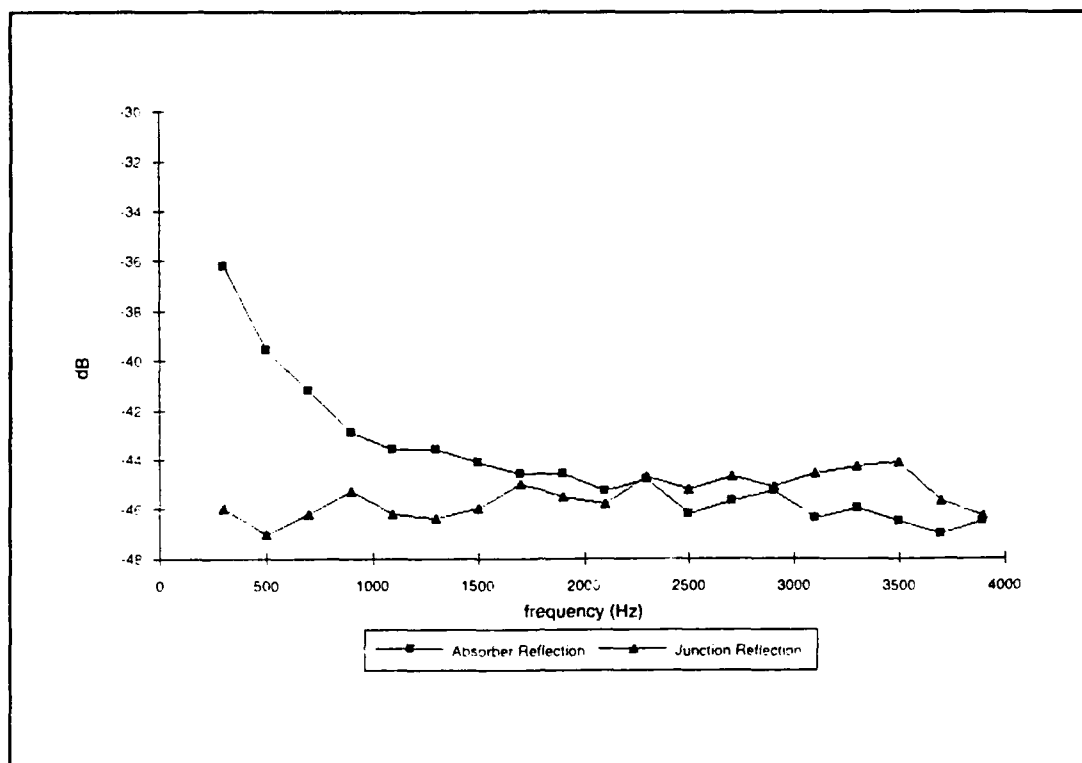


Figure 7: Absorber and junction reflection amplitude vs. frequency.

#### D. MICROPHONE PORTS

Four microphone ports for each of the six usable sections of pipe accommodate ENDEVCO series 8510B piezoresistive pressure transducers. The ports have a constant spacing of 2.50 ft. The microphones have a 0.150 inch face diameter and 10-32 mounting thread, and are 0.745 inches long.

Small rectangular mounting pads of aluminum plate 1.25 by 1 inches were made with a 2.377 inch outer diameter cylindrical cut along the longer length of the surface so that these pads would fit on the outer surface of the pipe sections (Figure 8). The metal thickness at the center of the pads was 0.228 inches. When added to the average

wall thickness of the pipe (0.210 inches) this gives a total span of 0.438 inches, which is the length of the microphone sampling stem. The pads were then fixed to the pipe sections with a high strength epoxy (Devcon Plastic Steel Epoxy). A 0.150 inch hole was drilled through pads and pipe walls and 10-32 threads tapped 0.30 inches into the hole. This leaves the last 0.138 inches nearest the pipe interior as a smooth 0.150 diameter hole to match the smooth end of the microphone stem. (Only 0.298 inches of the stem nearest the transducer body is threaded.) The result of this method was to ensure a flush microphone sample port that did not significantly change the interior volume of the pipe nor present an edge that might contribute to scattering of sound.

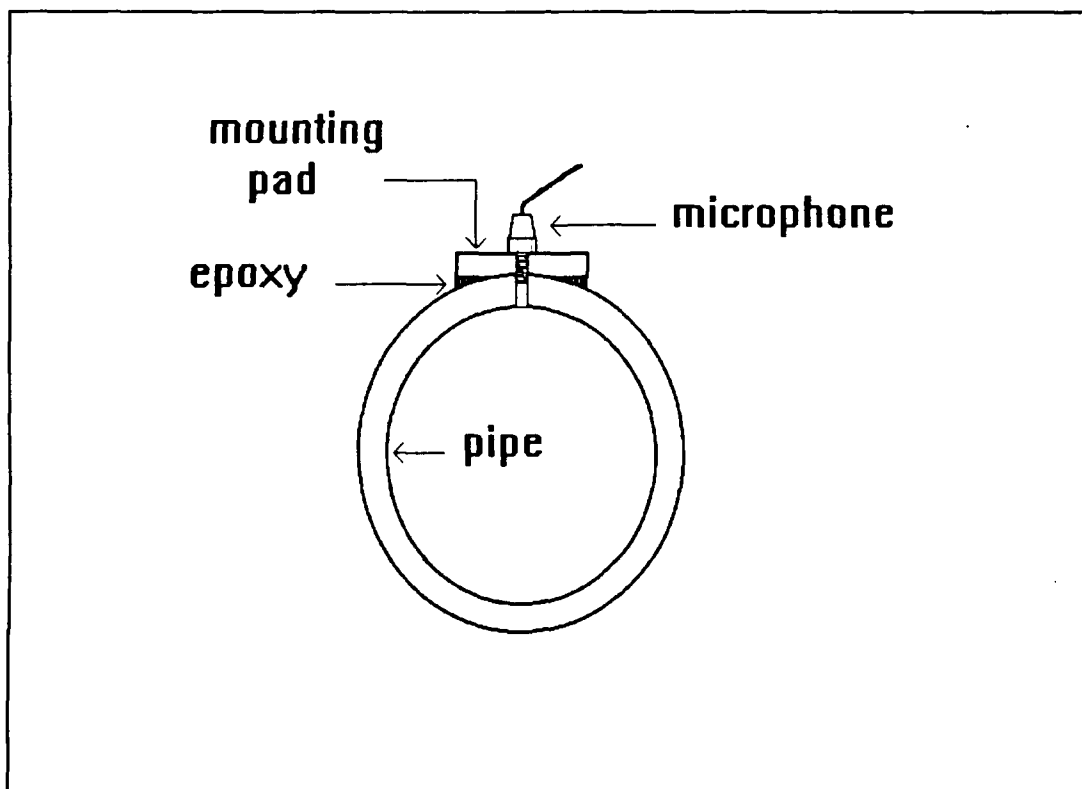


**Figure 8:** Microphone port installation.

Due to the high cost (\$500) of the microphones, one microphone per port is not feasible. The operator must move one or more microphones to gather a complete set of data. Ports without microphones are closed with plugs machined from 10-32 cap head screws.

## **E. EXPERIMENTAL TESTS**

The first test conducted was a check of the linear propagation loss down the length of the tube to see if it differed significantly from the expected exponential decay due to viscous losses at the pipe walls. Data was collected for four frequencies that span the intended operating range: 500, 1,000, 2,000, and 3,000 Hz. A monofrequency signal from a single driver was sampled at microphone ports placed ten feet apart down the length of the tube. The resulting data is plotted on a semi-log plot (Figure 9). The decays are nearly purely exponential and the attenuation constants agree with the expected values (Kinsler et al, 1982) to within 2% with  $\beta = 4.60 \times 10^{-4} \text{ sec}^{1/2}/\text{m}$ , appropriate to the apparatus.

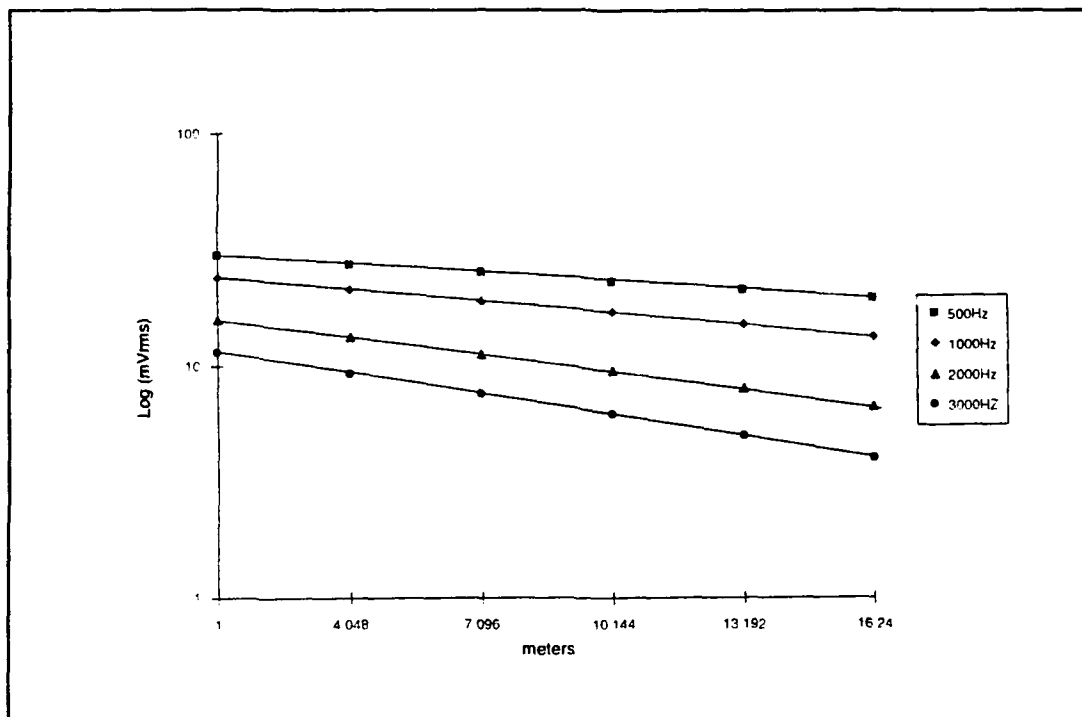


**Figure 9:** Exponential decay of linear waves due to viscous losses.

The second part of our test consists in determining if the sum and difference frequencies produced in the apparatus are the result of nonlinearities in the transducers or due to nonlinearities in the medium. Generation of sum and difference frequencies from intermodulation between the sources would be unsatisfactory for finite amplitude propagation experimentation with this device.

The spectrum produced by driving one source at 750 Hz and the other at 2000 Hz was sampled at six positions spaced ten feet apart. We recorded the intensity of the primary signals and their second harmonics, and the sum and difference frequencies. A comparison of Figures 10 and 11 will show that the sum and difference frequencies grow moving away from the sources.



Now consider  $(p_0 p_{\pm})/(p_{01} p_{02})$  as a function of  $x$  for the two frequencies  $f_1 = 750$  Hz and  $f_2 = 2000$  Hz. Using the value  $p_{01} p_{02} = 1.02\text{E-}6$  determined from the pressure values of the primary waves at 0.61 meters Figure 12 shows a comparison between theory (Equation II.C.18) and experimental values at different ports. If sum and difference frequencies are predominantly generated at the driver then they should attenuate exponentially down the tube due to viscous and thermal losses. However, if these frequencies increase in intensity moving away from the sources, then the nonlinearities are due to the medium. The growth of the sum and difference frequencies as a function of distance is shown for the six points sampled in Figure 12. It is clear that the sum and difference frequencies are produced as a result airborne nonlinearities. The 20% discrepancy between theory and experiment for the sum processes for distances greater than ten meters may be due to depletion of energy in the primary waves.

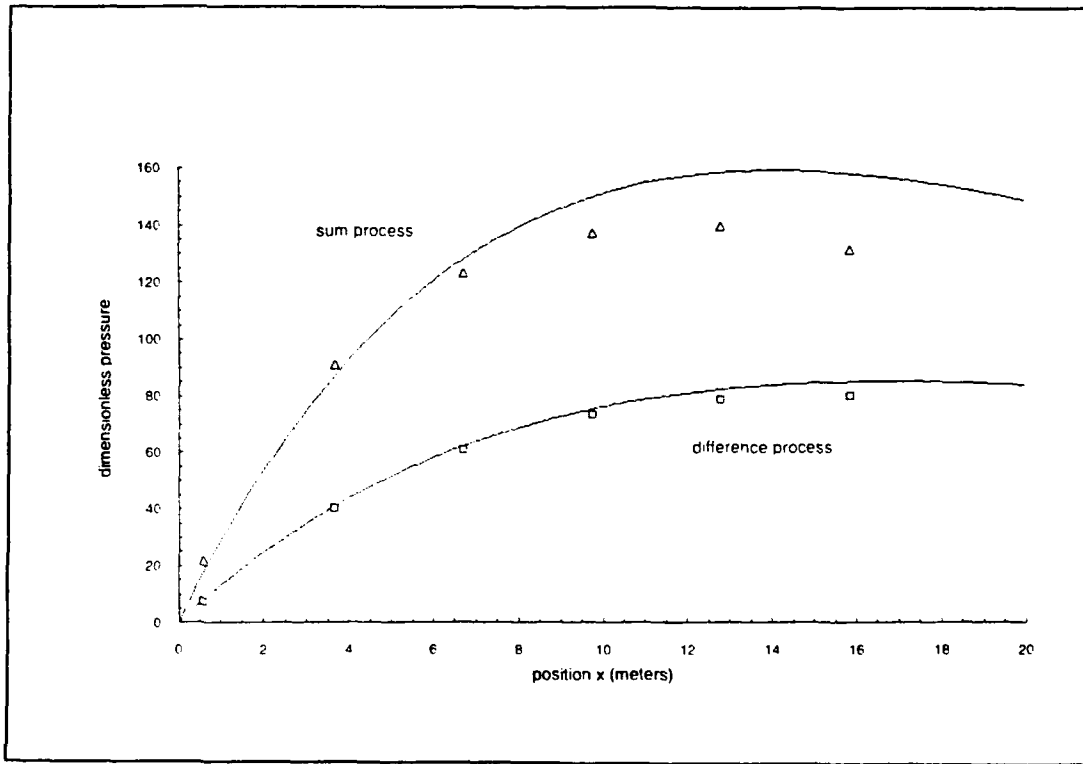


Figure 12: Experimental data points and theoretical curves for dimensionless pressure  $p_{\pm}p_0 / p_{01}p_{02}$  of the sum and difference processes.

#### IV. SUMMARY AND CONCLUSIONS

This thesis reports the design and construction of a high intensity travelling acoustic wave tube. Preliminary tests show that wall losses are the main cause for linear attenuation, that sum, difference, and harmonic generation can be accounted for mainly by nonlinearities in the medium, and that the absorbing end of the pipe substantially decreases the standing wave component of the acoustic field. These tests provide quantitative and qualitative limitations imposed by the apparatus for the applicability of the theory in Chapter II. Knowledge of the linear attenuation is required to interpret absorption measurements due to nonlinear interaction with a noise source. Linearity in the transduction was confirmed and is essential for any experiment that investigates nonlinear effects. Spatial modulations down the tube due to reflections at the end are unwelcome features that can hide an effect under investigation but these have been demonstrated to be very small for this apparatus.

The performance under these preliminary tests indicates that the apparatus is suitable for nonlinear acoustic investigations in forefront research as well as educational instruction. Attenuation of an acoustic signal due to noise in one dimension is an example of the forefront research possible with this apparatus. As for educational use, the study of shock wave development, sum and difference processes, and other nonlinear

acoustic topics taught in class, can be made more accessible using the apparatus reported in this thesis.

## REFERENCES

- Burns, Stephen H., 1971, "Rational design of matched absorbing terminations for tubes," *The Journal of the Acoustical Society of America*, v.49, pp. 1693 - 1697
- Cabot, M. A., 1983, *Nonlinear Acoustics in a Dispersive Continuum: Random waves, Radiation Pressure, and Quantum Noise*, Ph.D. Dissertation, University of California, Los Angeles
- Kinsler, Lawrence E., and others, 1982, *Fundamentals of Acoustics*, 3rd ed., John Wiley & Sons
- Newell, A. C., and Aucoin, P.J., 1971, "Semidispersive wave systems," *J. Fluid Mech.*, v. 49, pp. 593 - 609
- Riemann, B., 1858, *Über die Fortpflanzung ebener Luftwellen von endlicher Schwingungsweite*, Göttingen Abhandlungen, v. viii, pp. 43
- Rudenko, O. V., and Chirkin A. S., 1975, "Theory of Nonlinear Interaction Between Monochromatic and Noise Waves in Weakly Dispersive Media," *Sov. Phys.-JETP*, v. 40, pp. 945 - 949
- Stanton, T. K. and Beyer R. T., 1978, "The Interaction of Sound with Noise in Water," *The Journal of the Acoustical Society of America*, v. 64, pp. 1667 - 1670
- Stanton, T. K. and Beyer R.T., 1981, "The Interaction of Sound with Noise in Water II," *The Journal of the Acoustical Society of America*, v. 69, pp. 989 - 992
- Westervelt, Peter J., 1976, "Absorption of Sound by Sound," *The Journal of the Acoustical Society of America*, v. 59, 760 -764

## INITIAL DISTRIBUTION LIST

- |    |   |   |
|----|---|---|
| 1. | Defense Technical Information Center<br>Cameron Station<br>Alexandria, Virginia 22304-6145  | 2 |
| 2. | Library, Code 52<br>Naval Postgraduate School<br>Monterey, California 93943-5002  | 2 |
| 3. | Bruce Denardo<br>Physics Department, Code 63<br>Naval Postgraduate School<br>Monterey, California 93943-5002  | 3 |
| 4. | Andrés Larraza<br>Physics Department, Code 63<br>Naval Postgraduate School<br>Monterey, California 93943-5002   | 3 |
| 5. | Prof. Anthony A. Atchley, Code/Ay<br>Chairman<br>Engineering Acoustics Academic Committee<br>Naval Postgraduate School<br>Monterey, California 93943-5002 | 2 |
| 6. | LT Stephen J. Dorff, USN<br>806 Carpenter Road<br>Loveland, Ohio 45140  | 2 |
| 7. | Professor Karlheinz Woehler<br>Chairman<br>Physics Department, Code 63<br>Naval Postgraduate School<br>Monterey, California 93943-5002                    | 1 |